

Evaluation of factors affecting tibial bone strain after unicompartmental knee replacement

¹ Pegg, E.C, ² Walter, J., ¹ Mellon, S.J., ¹ Pandit, H.G., ¹ Murray, D.W., ³ D'Lima, D.D., ² Fregly, B.J., ¹ Gill, H.S.

¹ University of Oxford, Nuffield Department of Orthopaedics, Rheumatology and Musculoskeletal Sciences, Nuffield Orthopaedic Centre, Oxford, UK.

² Department of Mechanical & Aerospace Engineering, University of Florida, Gainesville, FL, USA.

³ Shiley Center for Orthopaedic Research & Education, Scripps Clinic, La Jolla, CA, USA.

Corresponding author:

Dr Elise Pegg

Address: University of Oxford,
Botnar Research Centre,
Windmill Road,
Oxford
OX3 7LD

Tel: +44 (0) 1865 227663

Fax: +44 (0) 1865 227671

Email: elise.pegg@ndorms.ox.ac.uk

Running title: Muscle Forces and Tibial Strains.

Abstract

Persistent pain is an important cause of patient dissatisfaction after unicompartmental knee replacement (UKR) and has been correlated with localised tibial strain. However, the factors that influence these strains are not well understood. To address this issue, we created finite element models to examine the effect on tibial strain of: (1) muscle forces (estimated using instrumented knee data) acting on attachment sites on the proximal tibia, (2) UKR implantation, (3) loading position, and (4) changes in gait pattern. Muscle forces acting on the tibia had no significant influence on strains within the periprosthetic region, but UKR implantation increased strain by 20%. Strain also significantly increased if the region of load application was moved >3 mm medially. The strain within the periprosthetic region was found to be dependent on gait pattern and was influenced by both medial and lateral loads, with the medial load having a greater effect (regression coefficients: medial=0.74, lateral=0.30). These findings suggest that tibial strain is increased after UKR and may be a cause of pain. It may be possible to reduce pain through modification of surgical factors or through altered gait patterns.

Keywords: Finite Element, Pain, Simulation, Unicompartmental, Knee

Introduction

While both total knee replacement (TKR) and unicompartmental knee replacement (UKR) are generally successful treatment options, unexplained pain remains an issue and is one of the most common causes of dissatisfaction and revision ^[1]. Persistent pain after knee replacement is also more common than after hip replacement ^[2]. The multifactorial nature of pain makes identifying the aetiology particularly challenging. Some authors have theorised that excessive strain within bone may stimulate nociceptor activity and cause pain ^[3; 4]. Simpson *et al.* correlated a typically painful region on the tibia, identified in patients after UKR, with an increased von Mises strain using finite element (FE) analysis ^[4]. However, the study only modelled articular contact forces, and loading from the muscles at their attachment sites on the tibia was not included.

Accurate estimation of muscle contact forces is difficult due to indeterminacy in the musculoskeletal system. This indeterminacy arises from having more unknown muscle forces than available equations from rigid body dynamics ^[5]. The most commonly used methods for estimating muscle forces omit inclusion of articular contact models and assume that muscles alone contribute to the net knee flexion-extension moment from inverse dynamics ^[6; 7]. Consequently, articular contact loads are not factored into the muscle force estimation process, which may result in inaccurate muscle force estimates. Through the use of an instrumented knee prosthesis, that can directly measure the force distribution between the condyles, Fregly *et al.* developed a 12 degree-of-freedom knee model that can resolve articular contact and muscle loads simultaneously ^[8].

This study uses FE simulations to examine the role that muscle forces, contact forces and surgical factors, play in determining tibial strain after UKR. Four hypotheses were tested: firstly that the addition of muscle forces to a FE simulation does not have a significant

effect on tibial strain; secondly, that implantation of a UKR increases tibial strain; thirdly, that malpositioning of the femoral component does not affect tibial strain; and fourthly, that tibial strain can be changed by gait modification.

Methods

Estimation of muscle and joint contact forces

A single subject (gender: male, BMI: 22.5, 83 years, neutral alignment) implanted with a force-measuring tibial prosthesis^[9] performed overground walking trials at a self-selected speed^[10; 11]. These trials included the subject's normal gait pattern and a medial-lateral trunk sway gait pattern intended to modulate medial contact force^[12]. These two gait patterns were selected to be used for the simulations which investigated the effect of gait on tibial strain. Contact forces applied to the medial and lateral sides of the tibial tray were collected simultaneously with ground reaction, surface marker motion, and electromyographic (EMG) data. Knee kinematics estimated from the marker motion data were adjusted such that medial and lateral contact forces calculated by an elastic foundation contact model of the subject's implant components reproduced the experimentally measured contact forces.

Muscle force estimates for thirteen muscles crossing the knee were generated using a subject-specific 12 degree of freedom musculoskeletal knee model and static optimisation^[8]. Tibiofemoral and patellofemoral contact forces were modelled using an elastic foundation contact (EFC) model^[13]. The knee model was identical to the one published by Lin *et al.*^[8] except that it was built in the OpenSim^[14] environment utilizing its inverse dynamics and moment arm analyses. Muscle attachments and wrapping surfaces were taken from a generic cadaver-based model^[15] and transformed onto the subject-specific geometry. Muscle force

was modelled as peak isometric force times activation, with activation modelled as simulated EMG shifted by a muscle-common time delay and raised to a muscle-specific power between 0.5 and 1 ^[6].

The static optimisation minimised errors between simulated and measured muscle EMG patterns (available for 9 of the 13 muscles modelled), and constrained the estimated muscle forces to balance the net superior-inferior force, varus-valgus moment, and flexion-extension moment at the knee. These net loads were calculated from inverse dynamics with contributions from contact forces eliminated ^[16]. Outputs from the musculoskeletal knee model were contact force magnitudes, directions, centres of pressure, and areas in the medial and lateral compartments, along with muscle force magnitudes, directions, and application points on the tibia. Included muscles were: the three vastii muscles, the rectus femoris, semimembranosus, semitendinosus, sartorius, gracilis, and tensor fasciae latae.

Preparation of the geometry

Using our previously validated methodology ^[17], computed tomography (CT) scans of a 60 year old subject (gender: male, BMI: 25.9) were segmented using Mimics software (version 14.1, Materialise, Leuven, Belgium) to create the tibial geometry. An iterative closest point (ICP) algorithm ^[18] was used to register this tibia model with the one used to calculate muscle forces (MATLAB, Version 7.10, MathWorks Inc., Massachusetts, USA), thereby allowing mapping of the muscle attachment sites. The tibia model was prepared for implantation of an Oxford UKR mobile bearing knee (Biomet UK Ltd., Bridgend, UK) in accordance with standard operative techniques ^[19] using Boolean operations (SolidWorks CAD software, version 2011-2012, Waltham, MA, USA). A sagittal cut to a depth of 4 mm below the medial plateau of the bone was made in line with the mechanical axis of the tibia and was positioned at the medial edge of the tibial spine. At the same depth anteriorly, a

transverse cut was made with a 7° posterior slope. The tibia was also truncated 100 mm below the medial plateau to reduce the overall model size. Use of a shortened tibial model has been validated previously ^[4].

The cuts resulted in two separate regions: the cut region and the main tibial region. In models which examined the tibia prior to UKR (hereafter referred to as the Native model), these two regions were bonded together using a tie constraint. For the simulations of the UKR, the cut portion was removed from the simulation and the main tibial region modelled with the components inserted (hereafter referred to as the Implanted model). For the Implanted model, a 1 mm cement gap was simulated between the tray and the tibia, and the tibial tray was implanted in the centre of the cut plateau. The bearing was positioned 1 mm from the wall of the tray and in the centre of the plateau along the anterior-posterior direction. The femoral component was aligned with the axis of the central peg normal to the surface of the tibial tray (Figure 1).

Finite element mesh definition

The two tibial regions were meshed separately; thus the mesh of the main part of the tibia was identical for all models. A mesh sensitivity study was performed on the Native model without muscle forces. Mesh sizes from 3.8 mm to 2.2 mm were assessed. Mesh convergence was defined as the point at which the von Mises strain was within 95 % of the strain of the next two smaller mesh sizes. This criterion was met by a mesh size of 2.4 mm, giving 70402 elements for the tibia (Figure 2). All the implanted Oxford UKR components were meshed using a mesh size of 2.0 mm, with a total of 14924 elements for the tibial component. Ten node tetrahedral elements were used throughout.

Boundary Conditions for the Finite Element Model

Static implicit FE models were created using ABAQUS (version 6.11, Simulia, Providence, Rhode Island, USA). A spatially varying value of Young's modulus (E) was used, with the value for specific bone regions being calculated from the Hounsfield units in the CT scan. A Poisson's ratio of 0.3 was assigned for all elements; the material property assignment was performed with Mimics. The equations used for the relationship were those defined and validated in a previous study ^[17]; 400 material assignments were used (E range, 0.01 GPa to 17 GPa, consistent with previous work ^[17]). All implanted components were modelled as linear elastic isotropic materials (Table 1). In the Implanted model, tie constraints were used for the tray-cement and cement-bone interfaces.

For the Native model, joint contact forces were applied directly to the tibial plateau. Joint contact forces measured experimentally varied in magnitude, direction, position, and contact area throughout the two gait cycles examined. A custom python script (Python version 2.7, Python Software Foundation) was written to identify elements within the calculated contact area (modelled as circular ^[20]) around the centre of pressure for the medial and lateral sides of the tibia; the load was uniformly distributed across this area. Muscle loads were also applied in the same manner using the areas specified by musculoskeletal model. Loads of appropriate magnitude and direction were applied to the tibia for the contact forces and muscle forces at each normalised location in the gait cycle (5% gait cycle intervals); these locations were modelled as a series of steps.

For the Implanted model, joint contact forces were applied to the tibial plateau using an analytically mapped field ^[21] with the same pressure distribution that would be caused by a femoral component loading a polyethylene bearing. The pressure distribution was calculated from a simulation including the bearing and the femur (Equation 1), where P_n is the force

applied to node n , P is the total medial load, and x_n is the radial distance of the node from the bearing centre.

$$\text{Equation (1). } P_n = P(-0.0014 x_n + 0.747)$$

During gait, the centre of the analytically mapped field was positioned at the centre of pressure given by the EFC model. If the centre of pressure would cause the bearing position to be beyond the tray wall, lateral movement was constrained.

Post-Processing

The von Mises strain (VMS) in two periprosthetic regions was found: a region defined on the exterior medial proximal cortex (Region A, 219 elements) examined in previous studies ^[4], and a region 2 mm lateral from the wall of the tibial tray where radiolucency is often observed (Region B, 123 elements),(Figure 1). As VMS is not a standard output for ABAQUS, it was necessary to modify the input file using a custom Python script. The VMS was calculated by dividing the von Mises stress for each element by its Young's modulus. The use of identical meshes for the main portion of the tibia enabled difference plots of the change in VMS (ΔVMS) to be created with a custom Python script.

Assessment of Difference

To evaluate the differences in VMS between the various FE models, the probabilistic statistical approach reported by Dar *et. al.* [22] was used. The error in load magnitudes calculated by the musculoskeletal knee model have been previously assessed [8]; the root-mean-squared (RMS) errors were 10 N for contact forces and 15 N for muscle forces. Given these error values, custom Python scripts were created which introduced equivalent artificial variability into the contact and muscle loads applied to the FE models, where the variability was assumed to be normally distributed. The Implanted model under normal gait cycle

loading was then run 40 times, each time with a different randomly created error for each load at each stage of the cycle. The variability in the results from these 40 tests was then used for statistical analyses.

The mean VMS within the specified regions (Regions A or B) was calculated for each of the 40 models and the 40 results treated as one dataset. Statistical analyses were then performed, using either a Kruskal-Wallis tests to compare multiple factors at once or a Mann-Whitney U test to compare two datasets. Spearman's rho was used to assess correlation and a multiple linear regression model was used to examine the significance of factors on the VMS (PASW Statistics, version 18.0.0, SPSS Inc, Chicago, USA).

Model Verification

To ensure that the contact loading method chosen did not affect the FE results, we examined different loading methods to assess their influence. The loading regimes used were; application of contact load through the femoral component and bearing (Verification Model A), application of contact load directly onto the tray using an analytically mapped field (Verification Model B), and application of contact load directly onto the tray using the same method as for loading the Native model (Verification Model C). No statistical difference was found in the results from the three methods (Figure 3). Therefore, the analytically mapped field was chosen for comparison with previous studies ^[4].

The use of a tie constraint to model the bonding at the cement/bone or cement/tray interface is a simplification, as these surfaces are predominantly bonded by a macro-geometric fit. A more complex model was created which used a friction coefficient of 0.3 between the cement and the tray [23] and a rough interaction between the cement and the bone (Verification Model D). No significant difference in strain was found between the model where the cement was tied and when a contact condition was used. Finally, a full

length tibial model was created to assess whether analysis of just the proximal portion changed the result (Verification Model E); no significant differences were found between the shortened and the full length tibial models.

Summary of Simulations

The simulations were organised into four groups designed to test the four hypotheses: (1) the effect of muscle loads on tibial strain, (2) the change in tibial strain after UKR, (3) the effect of bearing and femur (analytical loading) position on tibial strains, and (4) the change in tibial strain caused by varying gait pattern (Table 2). In simulations (2) and (3), the data at 16% of the normal gait cycle were used, as this point was when loading of the medial compartment was maximal. Muscle forces directly acting on the tibia were included in simulation 2 to 4, and to the relevant models for simulation 1. The effect of load position changes was examined using increments of 1 mm in the medial-lateral (ML) direction and 2 mm in the anterior-posterior (AP) direction. It was possible to move the load only 1 mm in the lateral direction due to the bearing being constrained by the wall of the tibial tray.

Results

During the majority of the normal gait cycle, the addition of muscle forces caused a localised increase in strain at the attachment sites on the tibia (Figure 3). This effect was particularly noticeable for the vastii and rectus femoris (via the patellar ligament) and the tensor fascia latae. However, the addition of muscles to the model did not cause any statistically significant changes in strain within the periprosthetic region (Figure 4) at any stage of the gait cycle (Table 3, $p < 0.05$).

After UKR an increase in strain was observed in two main regions: the corner between the sagittal and transverse cuts, and in Region A (Figure 5). The mean von Mises

strain in Region A after implantation significantly increased (Mann-Whitney U test, $p=0.0012$) by 24.6% (849.7 $\mu\epsilon$ native tibia, 1058.6 $\mu\epsilon$ implanted tibia). The strain within Region B decreased by 16.2% but this change was not significant (Mann-Whitney U test, $p=0.138$)

Movement of the loading position away from the centre, beyond 12 mm anteriorly or 10 mm posteriorly, caused a significant increase in the mean VMS in Region A (Kruskal-Wallis test, $p<0.035$). The strains increased to a 20% higher level in the posterior direction (14 mm posterior, 1716.6 $\mu\epsilon$) compared with the anterior direction (14 mm anterior, 1425.8 $\mu\epsilon$) (Figure 6a, S-Figure 6a - animation). Movement of the load position further than 3 mm medially from the centre significantly increased the mean von Mises strain (Kruskal-Wallis test, $p<0.008$). The strain increased by 900 $\mu\epsilon$ for every 1 mm of movement in the medial direction (Figure 6b, S-Figure 6b - animation).

A linear correlation was found between the joint contact load (both medial and lateral) and the von Mises strain in the periprosthetic regions of the tibia for both gait patterns examined (Figure 7). The Spearman's rho correlation coefficient was higher for the medial load (0.961) compared with the lateral load (0.792), but both were significant ($p<0.01$). Multiple linear regression showed that both medial and lateral load had an effect on the von Mises strain, but that the effect from medial load was greater (standardised linear regression coefficients: medial load = 0.739, lateral load = 0.298).

Significant differences in the VMS in Region A were found at certain stages of the gait cycle when comparing the two different gait patterns (normal gait and trunk-sway gait, Figure 8). Particularly significant differences were found in the VMS during push-off (40-50% gait cycle, $p<0.00004$); this was the stage when the VMS was maximal for both of the

gait patterns. At this stage the peak VMS during lateral trunk sway gait (1011.5 $\mu\epsilon$) was 6% lower compared with the normal gait pattern (1075.3 $\mu\epsilon$). Significant differences were also found at the end of terminal-stance (90-100% gait cycle, $p<0.03$); at this stage the peak VMS during lateral trunk sway gait (497.7 $\mu\epsilon$) was 50% lower compared with the normal gait pattern (248.3 $\mu\epsilon$).

Discussion

This study investigated four factors that could influence tibial bone strain, and therefore pain, following unicompartmental knee replacement. We found that UKR implantation, loading position, and gait pattern all significantly affected tibial strains; however, muscle forces acting directly on the tibia did not affect strains within the periprosthetic region.

This study failed to reject the hypothesis that the addition of muscle forces to a unicompartmental knee simulation did not have a significant effect on tibial strain within the periprosthetic region. However, the hypothesis was rejected for other regions in the tibial model. For studies which only need to consider the periprosthetic region of a unicompartmental knee, our findings indicate that the omission of muscle forces acting at their attachment sites on the tibia will not significantly affect the results.

Muscle forces have been shown to play an important role in measured strains within the hip [24-26], and the finding that muscle forces do not affect the periprosthetic region of the Oxford UKR highlights differences in muscular function between the two joints. The proximal femur is subjected to high bending forces due to the offset load, and the muscles surrounding the hip act to reduce these forces [24]. This function may not be as critical in the

tibia. It should also be considered that muscle forces implicitly contribute to the joint contact forces [27], and our study only removed the muscle forces from the attachment sites. Therefore, if the muscles act primarily to compress the joint, then no difference would be observed in tibial strains if muscular influence on contact force is not modelled. It is currently unknown whether this finding would hold true for a total knee replacement or a lateral UKR

The implantation of a UKR component increased the von Mises strain within Region A by 20% during normal gait. A previous study found a larger increase in the same region (40%) during a stair climbing load case which involved higher magnitude loads ^[4]. Whether this difference is due to the different load magnitude, the load condition, or the boundary conditions used is the subject of further study. A large increase in strain was also found in the corner between the sagittal and transverse bone cuts. This finding correlates with a study by Chang *et al.* [28], and it is not surprising that the corner acts as a stress-raiser. A high density of bone is often observed on radiographs in this region after the bone has adapted (approximately at one year post surgery) [29]. It is possible that the bone is remodelling in response to a high strain energy density [30]. Another consideration is whether this high strain could be related to subsidence of the tibial component, which is a possible complication after UKR. The cause of subsidence is unknown, but some studies associate it with poor underlying bone quality [31], incorrect component sizing [32], or excessive underhang of the tibial component [32]; all of which would increase the strain within the corner. Unfortunately the exact strain of a sharp corner cannot accurately be predicted using FE, it is necessary to include a realistic curvature. It is therefore not possible to draw any quantitative conclusions about subsidence from the present study; however, a

future study is planned which will determine the curvature at the tibial corner and analyse a variety of tibias with varying bone quality to examine this possibility.

The bearing of the Oxford UKR is completely mobile and follows the position of the femoral component due to the fully congruent spherical articulating surfaces [33]. As a result, the position of the bearing on the tray varies during gait, but surgical factors also affect the load location. In addition to femoral component placement, tibial tray positioning is important because the tray wall limits the bearing movement laterally. Correct tibial tray positioning has been shown to affect clinical outcome [4; 32]. For this reason, the positioning and orientation of the vertical cut should be correct and also the appropriate implant size should be used.

Positioning of the bearing, and therefore loading, in the anterior-posterior direction was not found to affect periprosthetic tibial strain significantly unless moved in excess of 10 mm posterior or 12 mm anterior from the centre. A fluoroscopic study examining Oxford UKR bearing translation found bearing motion to be predominantly posterior to the centre of the tibial component [34] with a maximum movement of 7 mm. Therefore AP motion is not thought to have a significant effect on tibial strain. However, in the medio-lateral direction, tibial strain increased the further medial the load was applied, and this effect became significant after only 3 mm of movement from the centre of the tibial component. This finding suggests that surgical factors which may force the bearing medially to a distance of more than 3 mm, such as medial placement of the femoral component, should be avoided. The bearing position may also be moved medially by the use of a small tray in a large patient, or by medial placement of the vertical cut; however, these factors were not examined in this study. Overhang of the tibial component beyond 3 mm has been shown to increase the risk of poor patient outcome [32] and increase the strain within the tibia ^[4]. An overhanging tibial

component would be more likely to shift the load medially due to the resultant medial positioning of the tray wall, assuming constant component size. It is therefore possible that the increased strain observed in previous studies is due to the shift in load position rather than the overhang itself.

Examination of the medial tibial von Mises strain during normal gait and trunk-sway gait revealed a significant correlation with both medial and lateral load. The correlation was stronger for medial load and multiple linear regressions revealed that medial load had a greater influence on tibial strain, though lateral load was also important. Based on this finding, if tibial strain relates to post-operative pain, then it may be possible to treat patients with pain non-invasively using gait modification techniques during the initial post-operative period to reduce medial load or to transfer load more laterally. Other methods which reduce joint contact force, such as a reduction in patient activity or use of an off loader knee brace [35] may also help. Gait modification has been researched primarily as a tool to reduce arthritic disease progression by reducing the external knee adduction moment, an indirect measure of the medial load [36]. The present study found a slight (6%) reduction in tibial strain for a trunk-sway gait pattern compared with normal gait which was significant for the FE data. However, trial-to-trial variability in the gait data was not taken into account. It may be possible to achieve greater reductions with different gait adaptations, such as using walking poles^[10].

The main limitation of this study is that the muscle forces applied are representative of only a very specific situation. The forces were calculated based on motion data captured from a subject implanted with an instrumented total knee replacement, and they therefore only represent an ACL deficient patient with an implanted knee. It has also been assumed that the loading conditions within the UKR, which are largely unknown, are similar to those

of a TKR. In this study, the load was applied directly to the bone rather than through cartilage, which may not represent the physiological situation. However, one of the indications for UKR is full thickness cartilage loss on the implanted side and thus we have assumed this representation to be reasonable for the one side; for the un-implanted side it is assumed this side is sufficiently far from the regions of interest not to influence the result, and this assumption was constant throughout all models. The implantation of the component into the bone was simplified and did not take account of pressurisation and forces during insertion; it is worth noting that these factors could have increased the strain further within the tibia. In addition to this, the cement thickness was assumed to be even around the implant; this assumption may have also introduced some error into the model.

When assessing statistical significance between models, an assumption was made that all of the variation within the models was caused by error in the load magnitude; therefore error in the load area and load position were not accounted for. Neither does this study account for the effect of patient factors such as gender, height, weight, age, or shape of the native tibia. The conclusions drawn from the gait cycle data were limited to only the two cases studied. Further work would be required to determine whether these conclusions apply to other scenarios as well. The registration of the muscle forces onto a different tibia may have also introduced some error, but the two subjects were of similar stature (Table 4), and the error would be consistent throughout because all results are comparisons of simulations using the same tibia.

In summary, this study assessed how a variety of factors affect tibial bone strain after UKR. Muscle forces applied to the attachment sites on the tibia were the only factor tested which did not cause a significant change. Strain was increased by implantation, by moving the implant loading medially, and by gait patterns resulting in higher medial loading. This

indicates that clinically, the incidence of pain after UKR might be reduced by improving surgical technique to ensure more lateral load positioning or by using gait modification techniques or a knee brace during rehabilitation to relieve symptoms.

Acknowledgements

The work was funded in part by NIH grant R01EB009351. Some of the authors have received funding from a commercial party, but this was unrelated to the present study. The authors would like to thank Mrs B. Marks (Nuffield Department of Orthopaedics, Rheumatology and Musculoskeletal Sciences, Oxford, UK) for her assistance with this study.

References

1. Pandit, H., Jenkins, C., Barker, K., et al., 2006. The Oxford medial unicompartmental knee replacement using a minimally-invasive approach. *J Bone Joint Surg Br* 88: 54-60.
2. O'Brien, S., Bennett, D., Doran, E., et al., 2009. Comparison of hip and knee arthroplasty outcomes at early and intermediate follow-up. *Orthopedics* 32: 168-168.
3. Brianza, S., Brighenti, V., Lansdowne, J.L., et al., 2011. Finite element analysis of a novel pin-sleeve system for external fixation of distal limb fractures in horses. *The Veterinary Journal* 190: 260-267.
4. Simpson, D.J., Price, A.J., Gulati, A., et al., 2009. Elevated proximal tibial strains following unicompartmental knee replacement—A possible cause of pain. *Med Eng Phys* 31: 752-757.
5. Kaufman, K.R., An, K.N., Litchy, W.J., et al., 1991. Physiological prediction of muscle forces—I. Theoretical formulation. *Neuroscience* 40: 781-792.
6. Lloyd, D.G., Besier, T.F., 2003. An EMG-driven musculoskeletal model to estimate muscle forces and knee joint moments in vivo. *J Biomech* 36: 765-776.
7. Buchanan, T.S., Lloyd, D.G., Manal, K., et al., 2005. Estimation of Muscle Forces and Joint Moments Using a Forward-Inverse Dynamics Model. *Med Sci Sports Exerc* 37: 1911-1916.
8. Lin, Y.-C., Walter, J.P., Banks, S.A., et al., 2010. Simultaneous prediction of muscle and contact forces in the knee during gait. *J Biomech* 43: 945-952.
9. D'Lima, D.D., Townsend, C.P., Arms, S.W., et al., 2005. An implantable telemetry device to measure intra-articular tibial forces. *J Biomech* 38: 299-304.
10. Fregly, B.J., D'Lima, D.D., Colwell, C.W., 2009. Effective gait patterns for offloading the medial compartment of the knee. *J Orthop Res* 27: 1016-1021.
11. Fregly, B.J., Besier, T.F., Lloyd, D.G., et al., 2012. Grand challenge competition to predict in vivo knee loads. *J Orthop Res* 30: 503-513.
12. Mündermann, A., Asay, J.L., Mündermann, L., et al., 2008. Implications of increased medio-lateral trunk sway for ambulatory mechanics. *J Biomech* 41: 165-170.

13. Bei, Y., Fregly, B.J., 2004. Multibody dynamic simulation of knee contact mechanics. *Medical Engineering & Physics* 26: 777-789.
14. Delp, S.L., Anderson, F.C., Arnold, A.S., et al., 2007. OpenSim: open-source software to create and analyze dynamic simulations of movement. *IEEE Trans Biomed Eng* 54: 1940.
15. Arnold, E., Ward, S., Lieber, R., et al., 2010. A Model of the Lower Limb for Analysis of Human Movement. *Annals of Biomedical Engineering* 38: 269-279.
16. Walter, J.P., D'Lima, D.D., Besier, T.F., et al., 2011. Feasibility of Highly Constrained Muscle Force Predictions for the Knee During Gait. In *ASME Summer Bioengineering Conference*. Pennsylvania, USA.
17. Gray, H.A., Taddei, F., Zavatsky, A.B., et al., 2008. Experimental Validation of a Finite Element Model of a Human Cadaveric Tibia. *J Biomech Eng* 130: 031016.
18. Besl, P.J., McKay, H.D., 1992. A method for registration of 3-D shapes. *IEEE Trans Pattern Anal* 14: 239-256.
19. Biomet, 2007. *Oxford Partial Knee Manual of the Surgical Technique*. Biomet UK Ltd., Bridgend.
20. Walker, P.S., Hajek, J.V., 1972. The load-bearing area in the knee joint. *J Biomech* 5: 581-589.
21. Feng, G., Qu, S., Huang, Y., et al., 2007. An analytical expression for the stress field around an elastoplastic indentation/contact. *Acta Materialia* 55: 2929-2938.
22. Dar, F.H., Meakin, J.R., Aspden, R.M., 2002. Statistical methods in finite element analysis. *Journal of Biomechanics* 35: 1155-1161.
23. Janssen, D., Mann, K.A., Verdonschot, N., 2009. Finite element simulation of cement-bone interface micromechanics: A comparison to experimental results. *Journal of Orthopaedic Research* 27: 1312-1318.
24. Duda, G.N., Heller, M., Albinger, J., et al., 1998. Influence of muscle forces on femoral strain distribution. *J Biomech* 31: 841-846.
25. Polgar, K., Gill, H.S., Viceconti, M., et al., 2003. Strain distribution within the human femur due to physiological and simplified loading: finite element analysis using the muscle standardized femur model. *Proc Inst Mech Eng [H]* 217: 173.
26. Stolk, J., Verdonschot, N., Huiskes, R., 2001. Hip-joint and abductor-muscle forces adequately represent in vivo loading of a cemented total hip reconstruction. *J Biomech* 34: 917-926.
27. Herzog, W., Longino, D., Clark, A., 2003. The role of muscles in joint adaptation and degeneration. *Langenbeck Arch Surg* 388: 305-315.
28. Chang, T.-W., Yang, C.-T., Liu, Y.-L., et al., 2011. Biomechanical evaluation of proximal tibial behavior following unicondylar knee arthroplasty: Modified resected surface with corresponding surgical technique. *Med Eng Phys* 33: 1175-1182.
29. Pandit, H., Jenkins, C., Beard, D.J., et al., 2009. Cementless Oxford unicompartmental knee replacement shows reduced radiolucency at one year. *J Bone Joint Surg Br* 91-B: 185-189.
30. Huiskes, R., Weinans, H., Grootenboer, H.J., et al., 1987. Adaptive bone-remodeling theory applied to prosthetic-design analysis. *J Biomech* 20: 1135-1150.
31. Vardi, G., Strover, A.E., 2004. Early complications of unicompartmental knee replacement: The Droitwich experience. *The Knee* 11: 389-394.
32. Chau, R., Gulati, A., Pandit, H., et al., 2009. Tibial component overhang following unicompartmental knee replacement—Does it matter? *The Knee* 16: 310-313.

33. Goodfellow, J.W., O'Connor, J.J., Dodd, C.A.F., et al., 2006. Unicompartamental arthroplasty with the Oxford knee. Oxford University Press, Oxford.
34. Pandit, H., Van Duren, B.H., Gallagher, J.A., et al., 2008. Combined anterior cruciate reconstruction and Oxford unicompartamental knee arthroplasty: In vivo kinematics. *The Knee* 15: 101-106.
35. Pollo, F.E., Otis, J.C., Backus, S.I., et al., 2002. Reduction of Medial Compartment Loads with Valgus Bracing of the Osteoarthritic Knee. *The American Journal of Sports Medicine* 30: 414-421.
36. Simic, M., Hinman, R.S., Wrigley, T.V., et al., 2011. Gait modification strategies for altering medial knee joint load: A systematic review. *Arthritis Care Res* 63: 405-426.

Figures

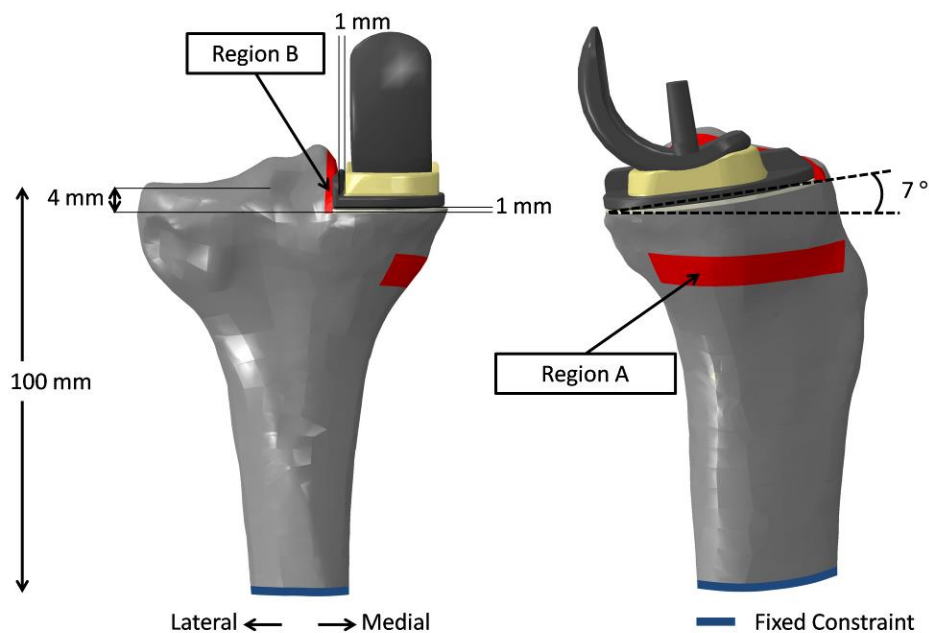


Figure 1. Illustration of the placement of cuts for the implantation and the position of the components. The periprosthetic analysis regions are highlighted in red. The anterior-posterior and the medial-lateral view are shown.

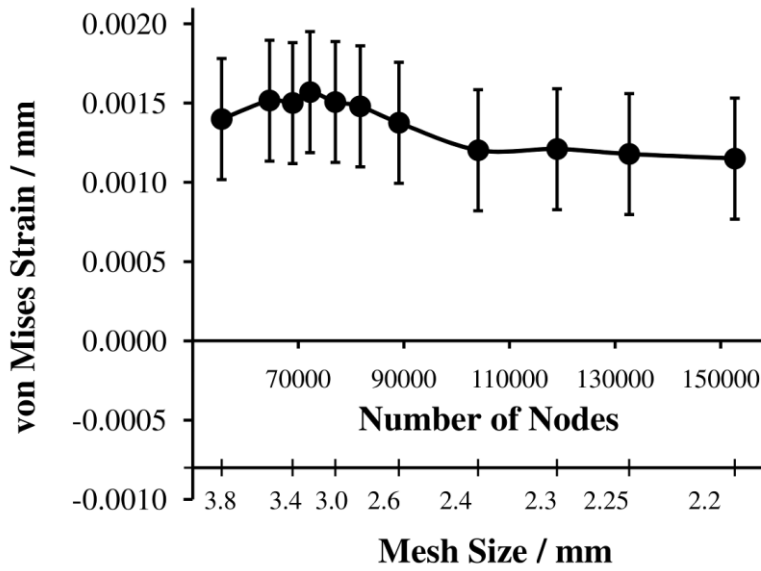
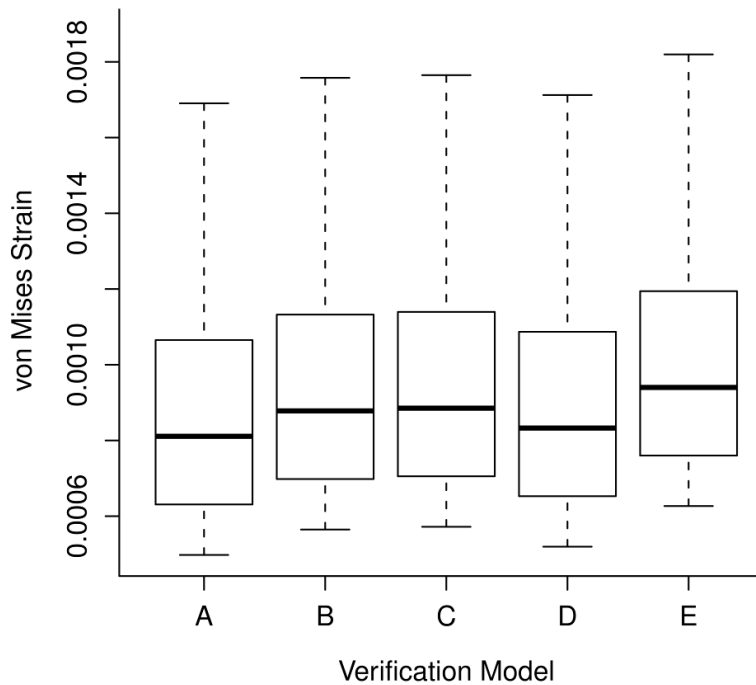


Figure 2. Dependence of the mean von Mises strain in Region A on the number of nodes in the model. The von Mises strain met the mesh convergence criteria at a mesh size of 2.4 mm (104,053 nodes). Error bars represent the standard deviation in the data.



Supplementary-Figure 2. Box-plot of the mean von Mises stress data within Region A for the five verification models. No significant difference was found between any of the datasets (Kruskal-Wallis, non-parametric test, $p > 0.05$).

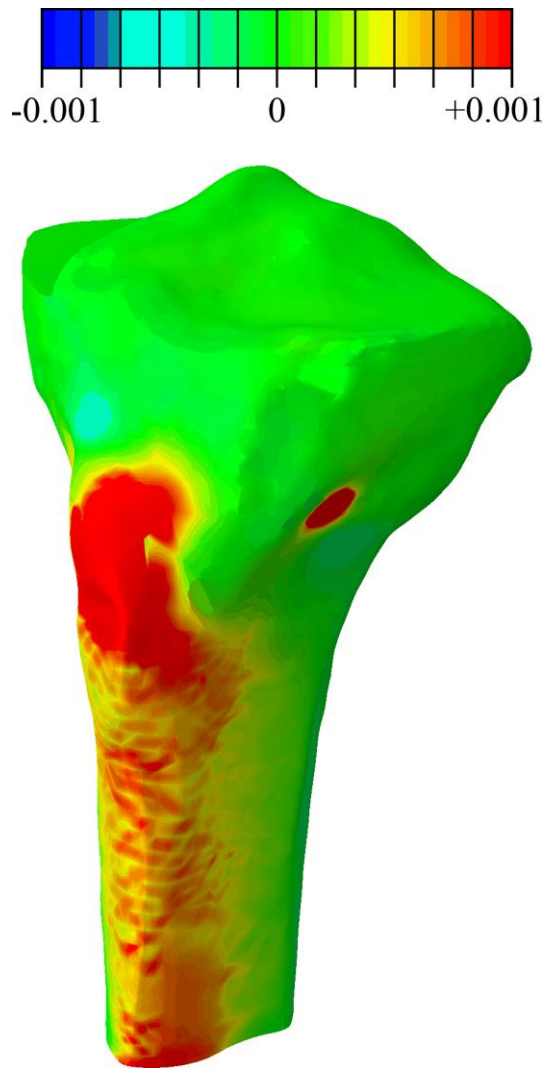


Figure 3. The distribution of ΔVMS is illustrated for loading conditions at 20% of the gait cycle.

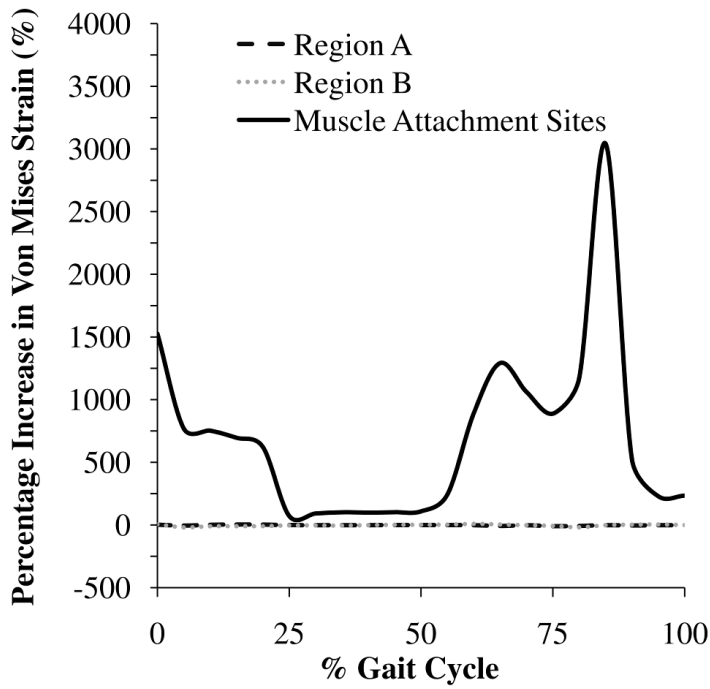


Figure 4. Average Δ VMS after the addition of muscle forces, results shown for; Region A, Region B and the muscle attachment sites. The analysis was performed with loading from a normal gait cycle, the mean values for the entire cycle are summarised.

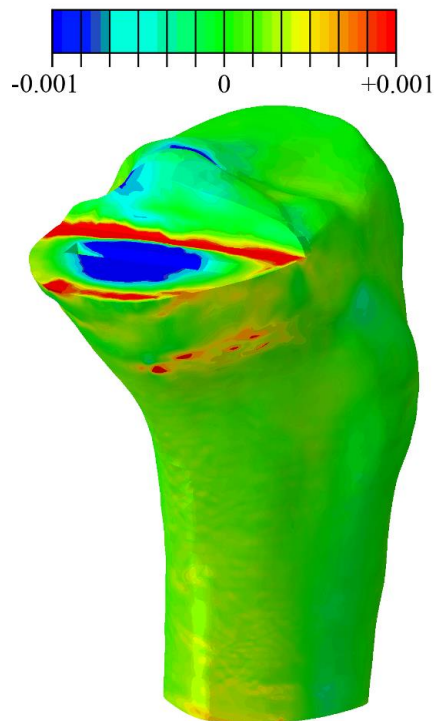


Figure 5. Regional change in von Mises strain after implantation.

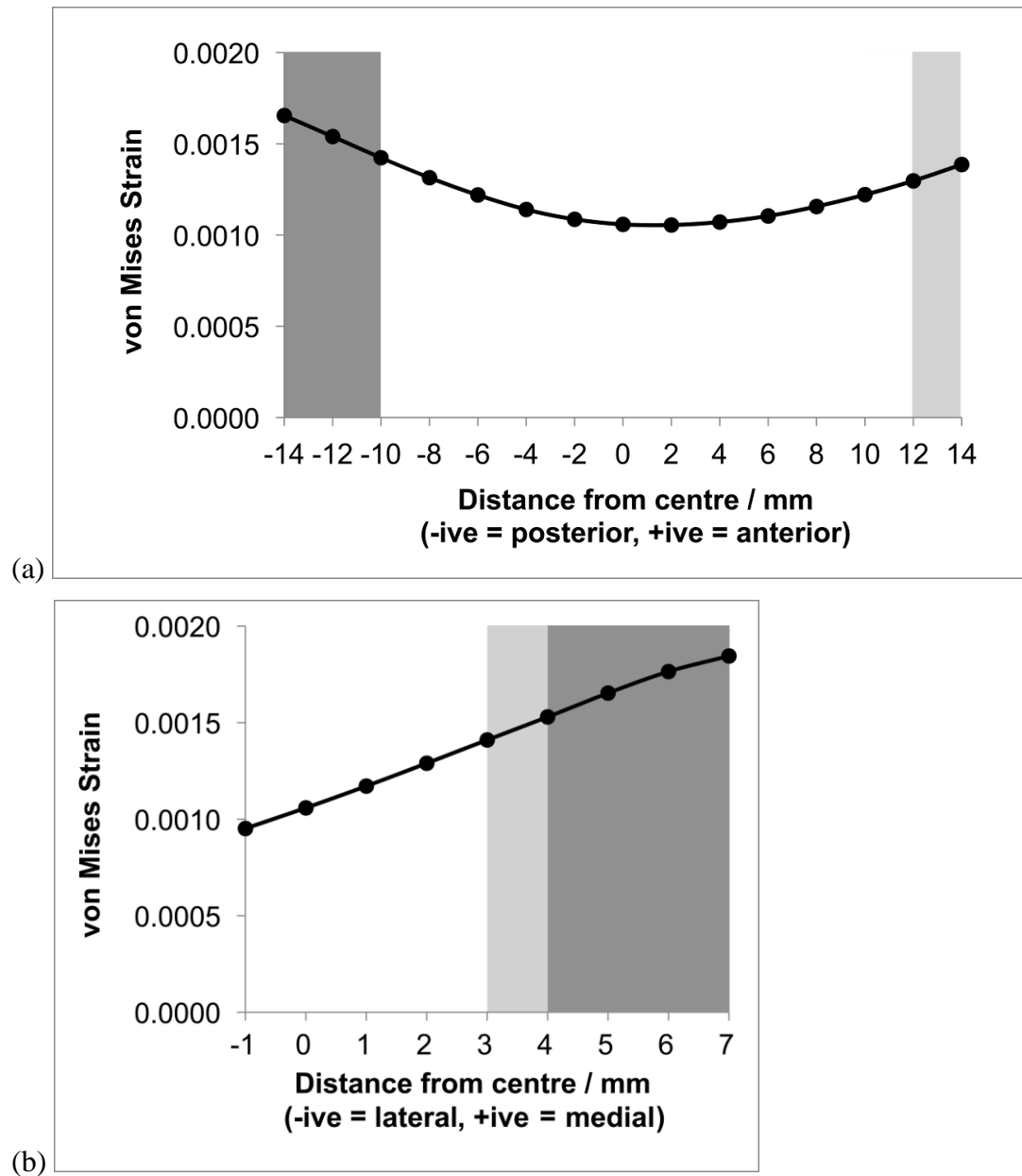


Figure 6. Illustration of the mean von Mises strain in Region A when the load position was moved from anterior-posterior (a) and from medial-lateral (b). Statistical significance between the von Mises strain at each distance compared with 0 mm distance are highlighted in light grey ($p < 0.05$) or dark grey ($p < 0.01$) as appropriate.

Supplementary-Figure6. Animation of the von Mises strain in the proximal tibial when load position was moved from anterior-posterior (a) and from medial-lateral (b) (see attached files).

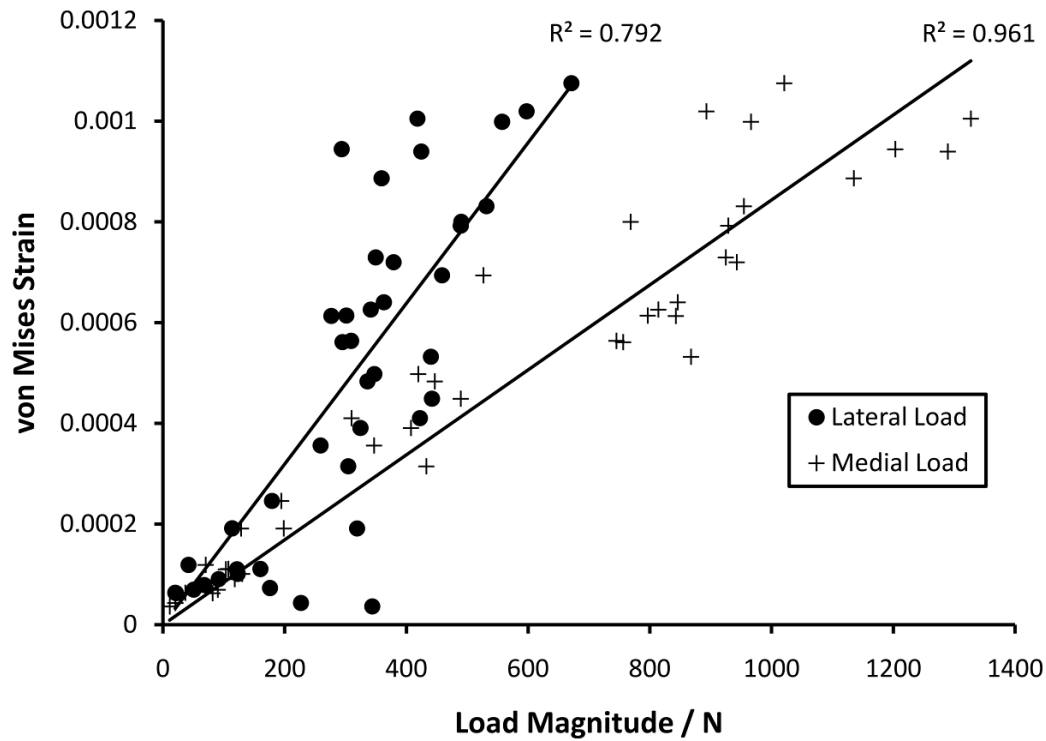


Figure 7. Curves illustrating the linear correlation between the medial and lateral load and the mean von Mises strain in Region A.

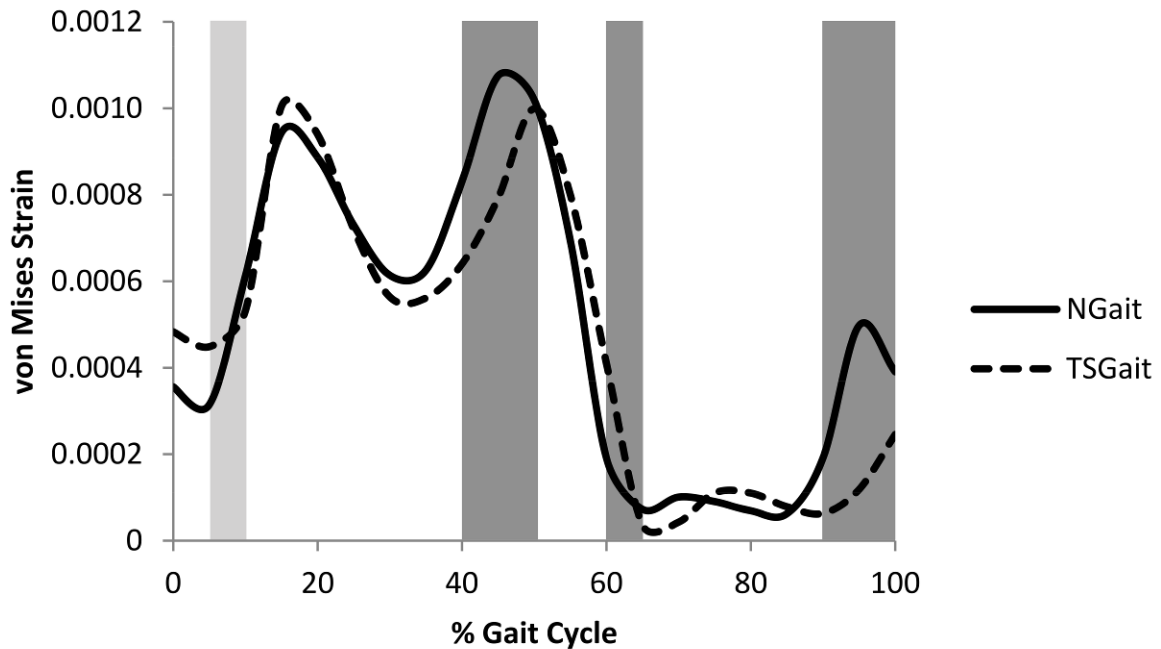


Figure 8. Variation in mean von Mises strain within Region A during normal gait (NGait) and lateral trunk-sway gait (TSGait). Statistically different results between the two gait trials, examined at each time interval, are highlighted in light grey ($p < 0.05$) or dark grey ($p < 0.01$) as appropriate.

Tables

Material	Part(s)	Young's Modulus (MPa)	Poisson's Ratio
PMMA	Cement	1940 [20]	0.40 [24]
UHMWPE	Bearing	940 [2]	0.46 [2]
CoCrMo alloy	Femur Tibial Tray	195000 [20]	0.30 [8]

Table 1. Material properties assigned to implanted Oxford UKR components.

Test	Models	Gait Pattern	Part of Cycle	Muscles	Load Movement
1	Implanted	Normal	All	With Without	Defined by gait
2	Implanted Native	Normal	16 %	With	Defined by gait
3	Implanted	Normal	16 %	With	Medial (+7mm)-Lateral (-1mm) Anterior-Posterior (± 14 mm)
4	Implanted	Normal Trunk-sway	All	With	Defined by gait

Table 2. Summary of the simulations performed; (1) the effect of muscle loads on tibial strains, (2) the change in tibial strains after UKR, (3) the impact of loading position on tibial strains and (4) the difference in tibial strain with varying gait.

% Gait Cycle	p value	
	Region A	Region B
0	0.738	0.718
5	0.565	0.327
10	0.718	0.429
15	0.512	0.341
20	0.799	0.602
25	0.799	0.758
30	0.678	0.659
35	0.718	0.698
40	0.718	0.718
45	0.718	0.779
50	0.779	0.738
55	0.738	0.698
60	0.779	0.678
65	0.779	0.799
70	0.799	0.779
75	0.718	0.799
80	0.758	0.779
85	0.799	0.799
90	0.779	0.779
95	0.758	0.758
100	0.718	0.799

Table 3. Mann-Whitney U results indicating the significance (p) of the von Mises strain between the model with, and without, muscle forces, at each stage of the gait cycle. The analysis was performed on the two periprosthetic regions. No significant difference was found between the data ($p < 0.05$) at any stage.

Model	Gender	BMI	Age / y
Musculoskeletal model	Male	22.5	83
FE simulation	Male	25.9	60

Table 4. Details of the subjects used for the musculoskeletal model and the FE simulations.